

MiniCOR: A Miniature Coronagraph for Interplanetary CubeSat

Clarence Korendyke, Damien Chua, Russell Howard, Simon Plunkett,
Dennis Socker, Arnaud Thernisien,
Naval Research Laboratory, Washington, DC
Contact: (202) 767-3144, ckorendyke@ssd5.nrl.navy.mil

Paulett Liewer, David Redding,
Jet Propulsion Laboratory, California Institute of Technology, Pasadena CA

James Cutler, James Forbes,
University of Michigan, Ann Arbor, Michigan

Angelos Vourlidis
Applied Physics Laboratory, Johns Hopkins University, Laurel, Maryland

ABSTRACT

Coronagraphs occupy a unique place in Heliophysics, critical to both NASA and NOAA programs. They are the primary means for the study of the extended solar corona and its short and long term activity. In addition, coronagraphs are the only instrument that can image coronal mass ejections (CMEs) leaving the Sun and provide critical information for space weather forecasting. We describe a low cost miniaturized CubeSat coronagraph, MiniCOR, designed to operate in deep space, which will return data with higher cadence and sensitivity than that from the SOHO/LASCO coronagraphs. MiniCOR is a six unit (6U) sciencecraft with a tightly integrated, single instrument interplanetary flight system optimized for science. MiniCOR fully exploits recent technology advances in CubeSat technology and active pixel sensors. With a factor of 2.9 improvement in light gathering power over SOHO and quasi-continuous data collection, MiniCOR can observe the slow solar wind, CMEs and shocks with sufficient signal-to-noise ratio (SNR) to open new windows on our understanding of the inner heliosphere. An operating MiniCOR would provide coronagraphic observations in support of the upcoming Solar Probe Plus (SPP) and Solar Orbiter (SO) missions.

OVERVIEW

Coronagraphs occupy a unique place in Heliophysics, critical to both NASA and NOAA programs. They are the primary means for the study of the extended solar corona and its short- and long-term activity. In addition, coronagraphs are the only instrument that can image coronal mass ejections (CMEs) leaving the Sun, and thus they provide critical information for space weather forecasting. One of the highest priority recommendations of the recent National Research Council Decadal Heliophysics study (http://www.nap.edu/catalog.php?record_id=13060) is to continue space-based coronagraphic observation beyond the lifetimes of the current missions with operating coronagraphs, Solar and Heliospheric Observatory (SOHO) and Solar-Terrestrial Relations Observatory (STEREO).

This paper describes the design of MiniCOR, a deep space, miniaturized coronagraph CubeSat. The design shows that a miniaturized coronagraph instrument on a CubeSat may obtain observations of comparable quality to that presently obtained by the Large Angle and

Spectrometric Coronagraph Experiment (LASCO) C3 coronagraph on SOHO. The design and mission operations scenario were specifically tailored to address the requirements of the EM-1 interplanetary space flight opportunity described in the NASA ROSES-2014 Heliophysics Technology and Instrument Development for Science (H-TIDeS) program and to meet two specific scientific objectives: (1) Improved measurements of CME kinematics and CME-shock standoff distance; and (2) Analysis of small-scale structures in the corona and solar wind. A MiniCOR placed at L1 could replace the current C3 coronagraph on SOHO/LASCO. A MiniCOR at L4 and L5 would allow optimal viewing of Earth-directed CMEs.

MiniCOR is a six-unit (6U) *sciencecraft* with a tightly integrated, single-instrument interplanetary flight system optimized for science. A single observation will consist of summed images (typically four but up to ten) with on-board cosmic ray scrub, providing a signal-to-noise ratio (SNR) improvement over SOHO of a factor of two to three. The active pixel sensor will operate continuously using a rolling curtain shutter; images will be recorded onboard for later selection and transmission

to the ground. Since MiniCOR is a single-instrument spacecraft, the operating cadence will be enhanced over that of SOHO/LASCO, which shared the data stream with multiple instruments. A minimal 3 months of operation will result in a unique data set to explore the inner heliosphere and provide ample opportunity to demonstrate the performance of the overall observatory. These advantages allow us to achieve the two major MiniCOR science objectives given above.

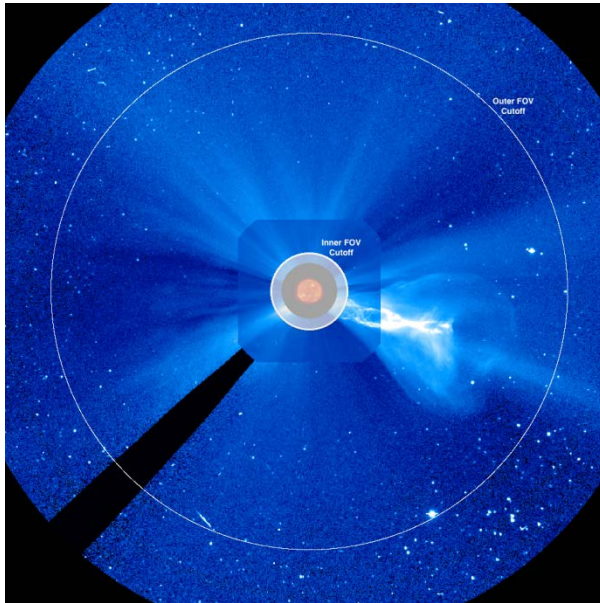


Figure 1. The MiniCOR FOV covering 2.5-20 R_s superimposed on the combined LASCO C2 & C3 FOV. The MiniCOR occulter (white semi-transparent circle) is comparable to the C2 occulter (2.5 vs. 2.2 R_s) but extends high resolution imaging into the C3 FOV. MiniCOR's plate scale is 19 arcsec/pixel compared to C3's 58 arcsec/pixel.

Figure 1 shows the MiniCOR field of view (FOV) imposed on an image from the SOHO/LASCO coronagraphs C2 and C3 (R_s = solar radius). Figure 2 shows the 6U MiniCOR spacecraft with the solar panels and occulter boom deployed. The MiniCOR coronagraph in the stowed configuration occupies a volume of ~2U, dramatically less than the equivalent of the LASCO C2 and C3 coronagraphs combined volume of 73.4U. The projected mass of the MiniCOR instrument is <3.6kg, much less than the STEREO COR2 coronagraph mass of ~13kg. The expected performance of MiniCOR will deliver higher quality data, at a faster cadence (~5 images/hour for LASCO C3 vs. ~15 images/hour for MiniCOR) over 60% of the C3 FOV with a factor of ~10 smaller volume than LASCO C3.

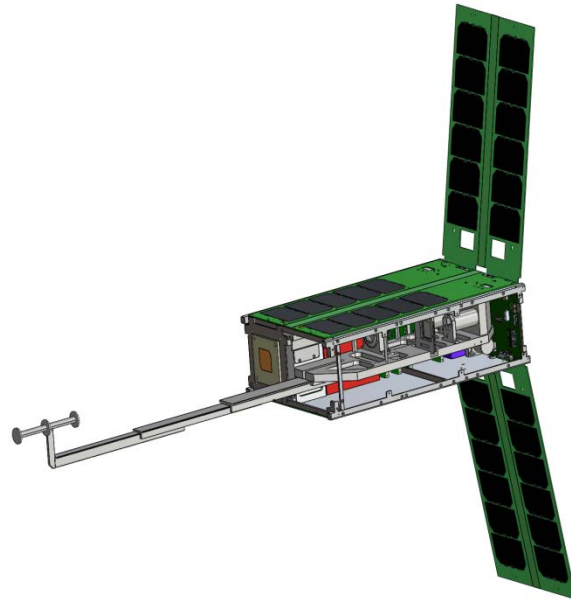


Figure 2. MiniCOR spacecraft shown with the deployed coronagraph boom and solar array. The spacecraft side panel instrument baffles have been removed to show the coronagraph optical train. The complete stowed MiniCOR instrument occupies a 2U volume and weighs 3.6kg.

MINICOR OBSERVING PROGRAMS

In Table 1, we outline a set of baseline observing programs that will return enough science-grade data to satisfy the scientific and technical objectives of the proposed EM-1 mission. The cadences in this table are for the summed images; the observing programs are consistent with the orbit and data rates assumed in the EM-1 proposal. MiniCOR can meet its mission objectives under a variety of telemetry and orbital conditions using a flexible set of electronics.

The MiniCOR camera design is a direct derivative of the Naval Research Laboratory (NRL) Wide-Field Imager for Solar PRobe Plus (WISPR) camera and has similar capabilities to the cameras of larger instruments, such as LASCO and SECCHI as described in Table 2. To achieve a significant increase in the SNR over present coronagraphs, a typical image will be a sum of four 20 sec exposures; onboard inter-comparison among the images will be used to eliminate the cosmic

rays and solar energetic particle hits. This allows MiniCOR to overcome one limitation of LASCO when viewing CMEs directed at the spacecraft: the images

can be swamped with energetic particle streaks. If pointing and observational considerations allow, the electronics has the capability to sum up to 10 images.

Table 1. MiniCOR Sample Observing Programs

Objectives	Solar Wind Small Scale Structure	CME Kinematics & Standoff Distance	Extended Phase Operations
Measurement	Power spectra, h-t ⁴ plots of solar wind blobs	h-t plots of CMEs and shocks	h-t plots of CMEs
Image Size (pixels)	1920 x 2048	1920 x 2048	960 x 1024
Binning	1 x 1	1x1	2x2
Compression	7.6	7.6	7.6
Spatial Resolution (arcsec pix⁻¹)	18	18	36
Cadence (min)	4	10	15
Total Daily Data Volume (MB)¹	430	194	33
Average Downlink Rate (Kbps)²	425	193 ³	21
Data Rate Capability (Kbps)²	400 – 3000	100	>20
Mission Days	0 – 20	0 – 100	100 – 150

¹Includes 5% CCSDS packer overhead, housekeeping telemetry at 1 min cadence, and a 15% overall margin.

²Two 8-hr downlinks with a 34m DSN antenna per week.

³Required rate to downlink full weekly dataset. Only specific event data will be downloaded to fit the downlink capability.

⁴ height-time (h-t)

TECHNOLOGY OVERVIEW

To achieve MiniCOR’s primary goal of operating a low-cost miniaturized science-grade coronagraph in deep space within the constraints of an EM-1 mission, we have designed a tightly integrated 6U sciencecraft that combines a science-grade 2U coronagraph with

sophisticated miniaturized systems for attitude control, deep space communications and other subsystems.

To achieve world-class performance in a 2U package, the MiniCOR coronagraph design has excellent optical performance, a small deployable (60cm) boom and incorporates a next generation Active Pixel Sensor (APS) detector. A comparison of MiniCOR’s

coronagraph to previous instruments is given in Table 2. MiniCOR will fully exploit the unique APS electronic shutter, the 16GBytes memory storage and superb spacecraft pointing capability to obtain an inner Heliospheric dataset with unprecedented sensitivity and temporal resolution. With a factor of 2.9 improvement in light gathering power over SOHO and quasi-continuous data collection, the MiniCOR observations will observe the slow solar wind, coronal mass ejections and shocks in the inner Heliosphere with sufficient SNR to open new windows on our understanding of the inner Heliosphere. Three months

of operations would result in a unique data set to explore the inner Heliosphere and provide ample opportunity to demonstrate the performance of the overall observatory. The MiniCOR team uses the high heritage Iris radio from the Jet Propulsion Laboratory (JPL)¹, combined with a fixed patch antenna and two eight- hour DSN passes per week, to meet the operational downlink and uplink requirements. A large 16GB onboard data store allows storage and selective downlink of the nearly continuous coronagraph observations.

Table 2. Coronagraph performance comparison: The unique MiniCOR sciencecraft permits an unprecedented ~100% instrument duty cycle with on-board storage of summed frames. Frames will be selected from the spacecraft mass storage for downlink.

Coronagraph	SOHO C2	SOHO C3	SECCHI COR2	MiniCOR
Field of view (R _s)	2.5-6	4-30	2.5-15	2.5-20
External occulter to objective lens distance (mm)	821	320	600	600
A1 to detector distance (mm)	714	570	635	378
Entrance aperture diameter (mm)	19	9	34	20
Focal length (mm)	388	77.6	120	115
Bandpass	C2 orange filter (540-640)	C3 clear filter (400-850nm)	660-740nm	475 – 750nm
Bandpass in nm	100 nm	450nm	90nm	275nm
Plate scale (arcsec/pix)	11.6	58	14	19
Detector	Front side illuminated Tek 1024x1024 CCD	Front side illuminated Tek 1024x1024 CCD	Back side illuminated E2V 2048x2048 CCD	Front side illuminated SRI 1920x2048 APS
light gathering power relative to C3 incl. detector correction	1.0	1.0	7.6	2.9
Standard Observing Program	Cadence: 12 min Images: 1 each Exposure time: 25s Duty Cycle: 4% Compression: 7.6	Cadence: 12 min Images: 1 each Exposure time: 45s Duty Cycle: 2% Compression: 6.2	Cadence: 10 min Images: 1 Exposure time: 4s Duty Cycle: 0.6% Compression: 4.0	Cadence: 4, 10 min Images: 4 summed Exposure time: 20 s Duty Cycle: 100% Compression: 7.6

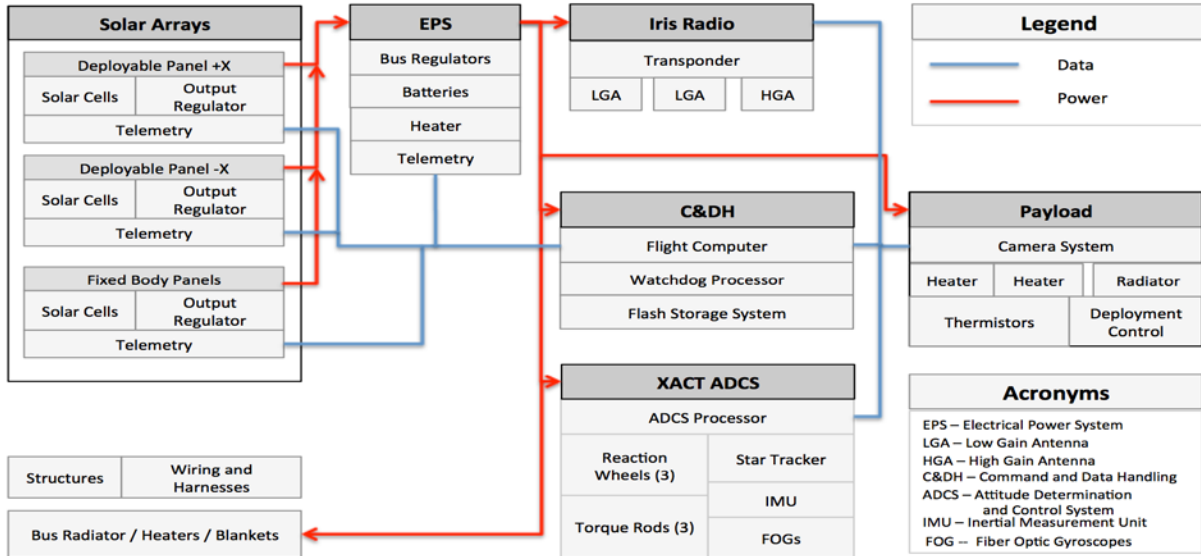


Figure 3. MiniCOR block diagram

Table 3. MiniCOR resource summary table. MiniCOR has excellent power/mass margins.			Figure 4. Stowed and deployed views of the MiniCOR spacecraft. The MiniCOR spacecraft is specifically designed to fit within a 6U structure. Top and side panels have been removed to show the compact stack of MiniCOR avionics and payload components.
Subsystem	Mass (kg)	Power (W)	
Payload	3.00	3.5	
ADCS (XACT, FOG)	0.78	0.66	
cabling/harness	0.1	0	
Propulsion	1.1	0.53	
Telecom subsystem	0.56	7.04	
Power subsystem	0.28	0.2	
Structure	0.48	0	
Thermal control	0.15	2	
Total	7.49	13.9	
Total w/cont	8.53	18.0	
Capability	14.0	24 BOL	

A block diagram of the proposed CubeSat hardware is shown in Figure 3. The deployed and stowed spacecraft configurations are shown in Figure 4. Table 3 gives the estimated mass and power of the major spacecraft subsystems with totals compared to capability. Ample mass and power margins allowed for considerable growth during the MiniCOR development program.

Coronagraph Description

The MiniCOR optical layout follows the design principles successfully used in developing the previous NRL coronagraphs. The optical prescription most closely follows the SECCHI COR2 instrument.² Table

2 shows the MiniCOR optical parameters. The optical layout is described in Figure 5. Two folding mirrors are required to meet the highly constrained volume requirements. The MiniCOR instrument field of view and the distance to the external occulter are nearly identical to SECCHI COR2. We expect to reach similar or better stray light ($\sim 3 \times 10^{-11} B/B_{\text{sun}}$ where B is brightness) in MiniCOR as achieved in the SECCHI instrument. The deployable boom design will closely follow the design of previous deployable booms constructed by NRL for the Solwind³, OSO-7 and previous sounding rocket coronagraphs. The design is readily manufactured with modest tolerances for a reasonable cost.

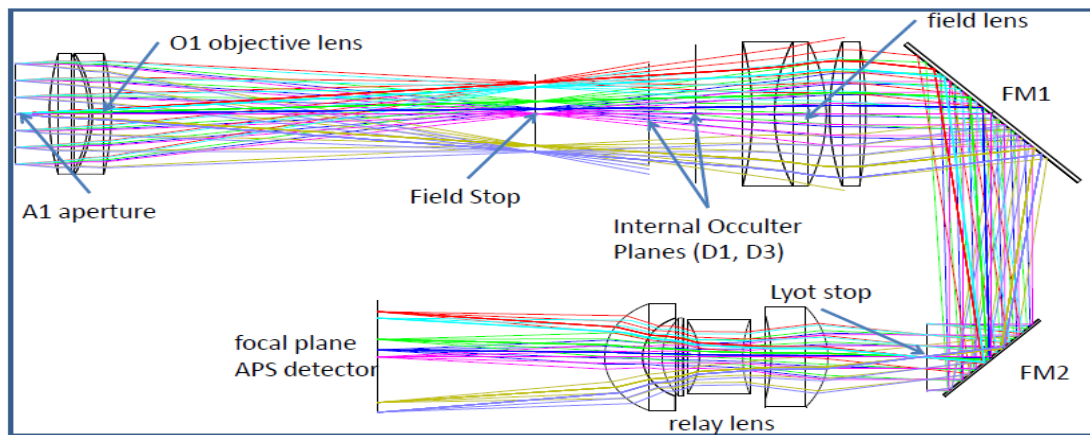


Figure 5: Coronagraph optical train fits within a 90x180mm box (outlined in blue). The objective doublet forms an achromatic image of the corona at the field stop and the last disk of the external occulter at the internal occulter. Residual diffracted radiation at the A1 edge remains a significant source of stray light. A field lens (O2) is placed directly behind the coronagraph field stop and internal occulter. O2 produces a high quality image of the A1 plane at the A3. The Lyot stop is placed in this plane to intercept the bright residual diffraction from the edges of the A1 aperture. If necessary, the MiniCOR team will intercept the doublet ghost (Lyot spot) at a point near this plane to maintain adequate stray light rejection. The relay lens (O3) reimaging the coronal scene onto the APS detector. A combination of long pass and short pass filters will be incorporated into the relay lens to define the instrument bandpass of 475 to 750nm. The expected MiniCOR image quality (~ 50 arcseconds FWHM) is a significant improvement over the C3 Nyquist limit of 120 arcsec.

Expected stray light suppression: The MiniCOR design is a traditional externally occulted Lyot coronagraph extending from the inner limit at $2.5R_s$ to the outer limit at $20R_s$. A coronagraph is a relatively simple telescope with the added complexity of several apertures and stops to eliminate sources of stray radiation. As shown in Figure 5, the MiniCOR optical design includes the necessary reimaging of the external occulter (EO) and the aperture A1 at the internal occulter and Lyot stop respectively, which allows removal of these instrumental stray light sources. As

shown in Figure 8, detection of the K-corona (solar) signal in the visible region of the spectrum is background noise limited by the F-corona (dust) beyond $2.5 R_s$. Externally occulted K-coronagraphs operating in the visible are designed to suppress the instrumental background below the unavoidable F-corona background. Instrumental background in the inner field of view is controlled primarily by the occultation subsystem. The MiniCOR and the SECCHI/COR2 solar occultation subsystems are comparable (see Table 2), with the most critical subsystem parameter, the inner field of view cutoff (IFOVCO), at $2.5R_s$ for both sensors. Thus the

MiniCOR inner field of view background should be comparable to COR2. The COR2 occultation background was measured pre-launch² over the 2.0-6.0 R_s half field interval. We used the measured COR2 background, corrected for EO-A1 separation, for the MiniCOR instrumental background prediction shown in Figure 6. At the focal plane, this level of stray light suppression is below the ambient K+F-corona and will not significantly affect the coronal observations as shown in Figure 7.

Boom description: The boom design follows the successful deployable boom used for the Solwind, OSO 7 and rocket-borne coronagraphs. Release will be accomplished with a pin-pulling paraffin actuator driven by the spacecraft electronics system. Each section will be pulled into its appropriate position with a constant force spring. Precision hardened steel locating pins will position each stage precisely. The stages will be driven along lubricated (Braycote), hardened steel rails. Caged, linear roller bearings will provide the necessary transitioning. A total error build-up of <0.5mm translation and <4 arcmin relative tilt have been allowed in the optical tolerance stack. A mechanical model will be constructed early in the program to retire residual risk.

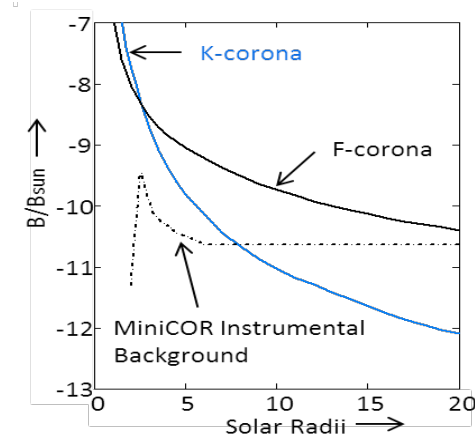


Figure 6: The brightness profiles, in units of mean solar brightness, of the unvignetted K-corona, F-corona, and the MiniCOR maximum expected instrumental background over the 2.5 R_s to 20 R_s field of view are shown. The stray light will be below the modeled background.

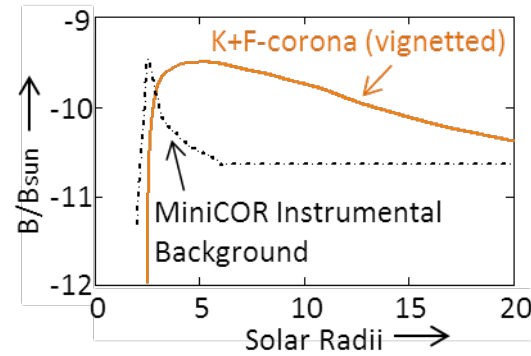


Figure 7: The MiniCOR vignetted K- plus F-corona profile and the instrument background incident on the detectors are shown. The maximum instrument background is below the natural scene K- plus F-corona profiles over the entire field of view from 2.9-20 R_s .

ACTIVE PIXEL SENSOR AND CAMERA ELECTRONICS DESCRIPTION

The MiniCOR detector will be a 1920x2048 format, 10 micron pitch 5T scientific grade active pixel sensor using a single die WISPR package. The detector die was fabricated in a dedicated lot run at the TowerJazz foundry for the SO/SoloHI and SPP/WISPR instruments, both under development at NRL.⁴ These detectors are ideally suited to the CubeSat application. The detector electronics require low operational power (<200mW operational), drive voltages ranging from -0.5 to 3.3volts and the detectors include a built in double correlated sample and hold capability. The devices are linear to within 1% over most of the 90,000 photoelectron dynamic range. The expected read noise is ~14 electrons (3σ) at high gain and will not affect the coronagraph data. The device MTF has been measured and is at the theoretical limit.

The MiniCOR Camera Electronics provide the functionality to read the 1920x2048 APS detector at 2Mpixels/second, perform Cosmic Ray Filtering (CRF) on each image acquired, perform image summing of up to 10 images, and provide image compression of the summed image. As shown in Figure 8, the MCE provides a straightforward power and digital communication interface (2Mbps with SPI format) to the CubeSat bus and payload. The baseline approach is to use a H-compress algorithm implemented within the FPGA to do image compression using 64x64 pixel blocks. The MCE can also bin pixels within a scrubbed summed image. The MCE will consist of a FPGA with a LVDS SPI interface and +3.3 and $\pm 5V$ voltage supply interface to the CubeSat bus. Local supplies of +1.5V

and $\pm 2.5V$ will be generated by the MCE. The APS detector interface with the MCE baseline consists of using an existing rigid-flex Detector Interface Board (DIB) assembly. Micro-coded logic controls the readout timing of the APS detector clock signals and video digitization. A 14bit ADC will allow the dynamic range of the APS detector to be fully exploited. Micro-power DAC's provide programmability of bias APS detector bias levels, video signal chain offset and calibration LED levels. Local analog telemetry is acquired and provided to the spacecraft in response to received command. The overall design of this card is very similar to the camera electronics presently under development for WISPR and SoloHI. The expected dissipated power of the camera electronics card is $<3.5W$.

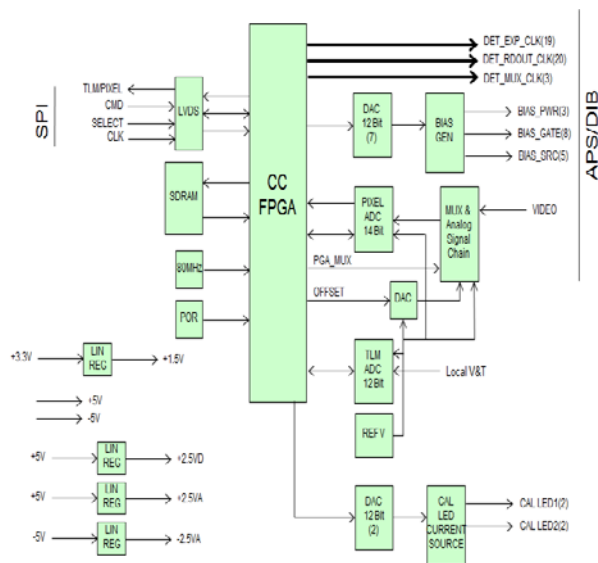


Figure 8. Block diagram of the MiniCOR camera electronics. The functionality of this card is very similar to the WISPR camera electronics presently under development at NRL.

ATTITUDE CONTROL SYSTEM

ACS Architecture: The attitude control system (ACS) architecture for MiniCOR is based on a standard 3-axis control configuration shown in Figure 9. ACS hardware and software are provided by Blue Canyon Technologies (BCT). The ACS hardware consists of two star trackers mounted orthogonally, a 3-axis gyro, and 3 reaction wheels. Each tracker (BCT nano-Star Tracker) is accurate to 6 asec with an NEA (noise equivalent angle) of 3 arcsec. The MEMs gyro that comes standard with the BCT bus is replaced with a

fiber-optic gyro, which has better bias and short-term stability. The short term stability of this fiber optic gyro is absolutely critically to obtaining the performance of the MiniCOR pointing system. Each of the 3 reaction wheels (BCT RWp15) has 15 mNms momentum storage and 0.6 mNm torque. Accumulated reaction wheel momentum is offloaded using a separate thruster-based system, which serves double-duty to remove tip-off rates. Expected pointing performance is summarized in Table 4.

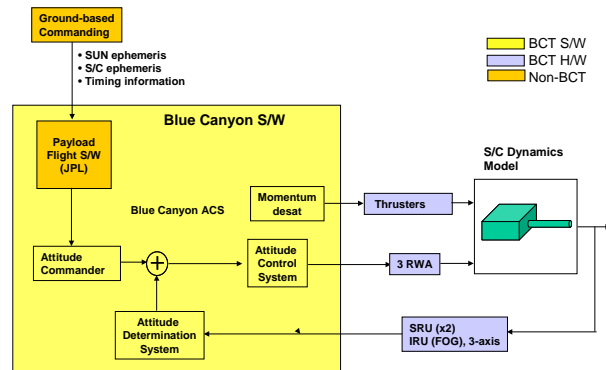


Figure 9. Block diagram of the MiniCOR ACS system.

Pointing Stability: JPL has conducted extensive analysis of the pointing stability. Attitude Determination System (ADS) stability is analyzed assuming that star trackers and gyros are combined using an optimized estimation filter. The filter is designed to offer the best balance of low- and high-frequency noise smoothing based on fast-observer theory. The line-of-sight (LOS) rotates at an attitude rate of about 1 deg/day due to orbital motion about sun. The stability performance of the resulting ADS estimate is scored over an ACS bandwidth of 0.5 Hz, and over time windows of 20 sec duration that is consistent with the intended exposure time. Reaction wheel disturbances produce most of the high-frequency errors. Due to lack of detailed data on the Blue Canyon RWp15 reaction wheels, pointing is analyzed using the comparable MAI-200 ADACS reaction wheels (CubeStaShop.com). Reaction wheel induced disturbances are scored over time windows of 20 sec duration, consistent with the intended MiniCOR exposure time, and multiplied by a factor of 10 as margin against unmodeled dynamics. A control error of 1 urad is allocated to cover control errors in excess of the knowledge error. Results indicate that MiniCOR's stability requirement of 10 arcsec is met with a value of 4.96 arcsec, yielding a 49.6% margin.

Parameter	Requirements	expected performance
Accuracy	60 arcseconds	52 arcseconds
stability over 20 second exposure	10 arcseconds	4.96 arcseconds
Optical resolution of the instrument is <36 arcseconds rms. The root sum square of the pointing expected performance contribute 0.33 arcseconds to the overall point spread function. The pointing performance stability can substantially exceed the requirement (up to ~60 arcseconds) and still maintain comparable imaging performance to LASCO C3.		

Table 4: MiniCOR ACS and requirements and expected performance.

CUBESAT SPACECRAFT SYSTEMS

The MiniCOR mission will leverage extensive heritage from previous successful missions with a team experienced in multiple CubeSat missions and launches. The ACS is a key enabler for this mission and is described above. Two additional fundamental enablers are the communication system capable of deep space communication and tracking and the propulsion system for attitude control. These are described below along with the remaining subsystems.

STRUCTURE

The 6U CubeSat structure is a modular 10 cm × 10 cm × 34 cm exoskeleton frame developed by the Michigan Exploration Laboratory (MXL). It is aluminum with hard anodized rails. 6U PPOD deployers are still in work and the structure will be adapted to the relevant launch mechanism used. Two rigid sidewalls have four PPOD interface railings that extend along the 34-cm edge. Modular rails connect the sidewalls to complete the exoskeleton. The frame provides standard mounting surfaces for the core bus technology as well as flexible payload mounting options.

THERMAL CONTROL

Thermal control is required for proper payload operation and heat management from the Iris radio. The payload requires an operating range of 0-40°C. A dedicated passive radiator is used to cool the APS (-55 to -75 °C) to its operating temperature. The present design includes active thin film payload structural heaters (2W), detector trim (0.25W) heaters and decontamination heaters (5W). A radiator will dump excess heat from the payload. A 9 cm by 18 cm radiator will be attached as a thermal sink for the Iris radio. The 18W of surplus heat will be removed from the satellite

with the radiator to maintain nominal temperatures. Thin film heaters attached to the Iris radio enclosure will provide heat if necessary.

COMMAND AND DATA HANDLING

MXL's command and data handling (C&DH) subsystem provides the spacecraft with the necessary central processing and data storage capabilities for both the flight system and science data. C&DH data storage system can handle greater than 16 GB of data on discrete flash and SD-card based flash memory. MinCOR can store up 28 days of continuous observations onboard.

The resources required for payload commanding are minimal. A specialized command set provides control of payload deployment and heaters. Low-level binary commands are passed to the payload for imaging configuration. Additional commands place the payload into flight mode, safe mode, test mode, and off. The C&DH has a combination of low-power embedded processors based on the Texas Instrument MSP430 and a high speed Atmel AT91SAM9G20 processor running at 400 MHz with 128 MB of static random-access memory, and 512 MB of NAND flash memory. The C&DH communicates to other subsystems with inter-integrated circuits (I2C) buses, serial peripheral interface buses, and dedicated universal asynchronous receiver/transmitter connections.

An independent hardware "watchdog" system monitors C&DH performance and power-cycles the flight system if necessary. It also can receive direct commands through the transceiver for power cycling. The watchdog system itself is periodically power-cycled by a HEF4521B timer to clear transient faults. Fault protection is also implemented with a redundant SD card and current-limiting hardware in the power subsystem and payload module.

MXL flight software and procedures are derived from previous UM missions that have analogous hardware and payload interfaces such as M-Cubed and GRIFEX. About 50% of the software is directly inherited. The operating system is Linux (2 MB); the C&DH routines (6 MB) are a collection of C and scripted language applications that run the satellite. This flight software easily fits in the available storage in the C&DH. Modified code and executables can be uploaded to the satellite on orbit.

PAYLOAD INTERFACE MODULE

The payload interface module (PIM) provides a custom interface between the C&DH and the payload. The primary interface to the payload is a synchronous serial interface that enables 1–2 Mb/s data and command

transfers. Four analog voltage lines from the payload enable temperature monitoring by the C&DH through the PIM. The unregulated battery voltage, 3.3V, and 5.0V bus voltages are provided to the payload through current-limiting and current-monitoring switches. Supplemental voltages are provided for the detector electronics as required. The switches shut off during current spikes. This provides protection against transient single event upsets and the capability to completely power cycle the payload. Isolation circuitry (using standard Texas Instruments isolation chips) prevents improper current back flows and any voltage level shifting. This enables the payload to be powered off and electrically isolated from the bus (the grounds are still connected).

POWER SYSTEM

The power subsystem combines solar cells and batteries to provide power under worst-case conditions. Two



Figure 10: HGA patch antenna array and LG “receive” and transmit antennae at the rear of the spacecraft.

deployable solar panels are released with a spring and hinge mechanism to a fixed angle set with a customized hinge- stopping bracket. The angle, the only design change between the two solar panels, is optimized prior to launch for the chosen orbit. There are four body-mounted panels as well to provide power during maneuvers and detumbling post launch. Each solar panel has twelve EMCORE third generation triple junction (ZTJ) cells with 29.5% efficiency strung in series on each side. The panels each have an independent buck regulator to provide power conversion to the bus voltage and track peak power production. A breakdown of the power budget is given in Table 3. During high current consumption modes (e.g., DSN contacts), a battery system provides supplemental power. Four Panasonic 18650 lithium ion cells store 6,200 mAh at 8V. Power is distributed to the satellite through low-noise, low-ripple bus regulators at 3.3V and 5.0V. Voltages, currents, temperatures, and

efficiencies of all regulators are monitored. Bus voltages are distributed to all subsystems and, as necessary, local point-of-load regulators. The buses and subsystems are switchable (on/off) and current-limited.

COMMUNICATION SYSTEM

The Iris radio from JPL coupled to a high gain antenna and two low gain antennas will provide high and low rate communication and tracking in the near Earth and deep space environment. A link budget with appropriate performance margins was developed..

Iris Radio – The MiniCOR design incorporates the second-generation Iris radio from JPL which is deep-space and CubeSat compatible. The first version was developed for JPL’s INSPIRE “First CubeSat to Deep Space” mission and delivered to that project, ready for flight, on June 30, 2014. DSN compatibility was formally verified at DSN Test Facility 21. This transponder operates on any channel in the deep space or near Earth X-Band (downlink 8.4 – 8.5 GHz) providing an uplink at 1000 bps BPSK on 16 kHz subcarrier with FireCode (spacecraft reset) support and downlinks in the range 62.5 to 25600 bps on subcarriers (nominal 25 kHz, others available) or direct on carrier with or without residual carrier for navigation purposes. Iris provides navigation support through the Doppler data type, coherently reproducing the uplink frequency and phase at the standard X-Band 880/749 turnaround ratio. It also supports the ranging data type by non-regeneratively transponding ranging tones or codes within a 1.5 MHz bandwidth. The Iris for INSPIRE was built with commercial, off the shelf (COTS) parts for a nominal 90 day mission up to a few million km from Earth. Iris supports two sets of transmit and receive antennas and has a mass of 0.4 kg.

A significant revision of the Iris transponder is now under way to produce a “Version 2 (V2)” unit that is suitable for longer duration missions, up to 2.5 years, in deep space through radiation hardening, improved power input to radio power output efficiency, better thermal design, and additional signaling features such as Delta-DOR navigation support and a larger selection of uplink command rates. The resulting V2 transponder will put out 2 Watts of RF power and feature a receiver sensitivity of better than -125 dBm. DC power input for full transponding will be 20 Watts or less with lower power receive-only modes available. The stack is approximately 0.4U (9.1x9.8x4.0 cm).

The Iris V2 transponder includes two low gain antenna (LGA) boards with approximately hemispherical coverage that can be placed on diverse locations on the spacecraft exterior. Each LGA board has one “receive” and one “transmit” antenna. The two transmit and two

receive paths can also be configured to be used with MiniCOR's high gain antenna (HGA). Figure 14 shows the HGA and one set of the hemispherical LG "receive" and "transmit" antennae.

High Gain Patch Antenna Array. A patch antenna array on the rear of the satellite will provide sufficient link margin for high rate communication at expected distances. The array is approximately a 100 cm² patch 15dB X-band antenna with 16 ~1 inch patches as shown in Fig. 10. It will be provided by Antenna Development Corporation. During DSN passes, the high gain antenna would be pointed directly to Earth.

COLD GAS PROPULSION SYSTEM

The momentum unloading system chosen for MiniCOR is a cold gas thruster that uses an additive manufacturing (3D printed) tank. The thruster is the same design that is being flown on JPL's INSPIRE mission (hereafter referred to as the INSPIRE thruster) which was developed at the University of Texas.

The propulsion system uses an inert liquid refrigerant as a propellant that provides simple, low cost, and safe operation. The 3D printed tank can be easily reconfigured into various shapes and volumes, making efficient use of the volume on CubeSats.

CONCLUSIONS AND FUTURE WORK

The MiniCOR design shows that: (1) existing instrumentation for space weather can be miniaturized and still give performance comparable to previous instrumentation and, (2) capable interplanetary CubeSat platforms meeting rigorous performance requirements can be designed. If successfully demonstrated, there are significant implications for NASA's future research and mission strategies. Imaging telescopes could be accommodated on almost any conceivable spacecraft platform and mission design because their resource allocations (volume, power, mass) will be on par to those of *in-situ* instruments. The cost of instrument development may be significantly reduced, especially when the science objectives do not call for breakthroughs in spatial resolution or image cadence. This would be particularly beneficial for operational or research-to-operations mission concepts. There exist several mission concepts where the new science relies on the unique vantage point (e.g., Solar Polar Imager or a mission to the L₅ Lagrangian point) and not on high spatial resolution or cadence. On the other hand, such unique vantage points impose severe restrictions on instrument mass and power and therefore, instrument concepts such as MiniCOR can enable such missions. A small spacecraft similar to MiniCOR could be part of a constellation of small satellites achieving the goals of existing larger mission concepts, such as the L₅ Space

Weather Sentinel Concept described in the report "Small Satellites: A Revolution in Space Science" (<http://www.kiss.caltech.edu/study/smallsat/KISS-SmallSat-FinalReport.pdf>) and in Liewer et al. (2014)⁵. Finally, operational applications of CubeSat and small satellite introduce the need for a family of commercial CubeSat components using a higher grade of parts, quality assurance and incorporating significant life testing.

Although MiniCOR presently has no identified launch opportunity, the MiniCOR team will continue to develop this technology. We will focus principally on the ACS hardware which would benefit by further testing and characterization. JPL has begun an institutionally funded CubeSat ACS testbed activity, that will test key ACS components, and could then test the prototype ACS system performance as a whole using air bearing tables, projected star references and other facilities. Component and system-level hardware testing will provide subsystem and system-level performance data beyond what is currently available from the vendors; this data will be shared with the vendors. It will address a range of commercial-of-the-shelf (COTS) ACS technologies, including hardware testing of CubeSat reaction wheels, gyros, and star trackers of the specific type used by MiniCOR. Other design possibilities will be explored. We will look at adding a 4th reaction wheel so speeds can be controlled to avoid exciting structural resonances. We will look at upgrading the currently proposed 15 mNms RWAs to 100 mNms RWAs for increased control authority.

ACKNOWLEDGEMENTS:

The authors gratefully acknowledge the institutional support at the Jet Propulsion Laboratory. The authors also gratefully acknowledge the ONR 6.1 basic research support of this development work at the Naval Research Laboratory. The work of PL and DR was conducted at the Jet Propulsion Laboratory, California Institute of Technology under a contract from NASA. This work would not have been possible without the encouragement and support of numerous colleagues at various institutions.

REFERENCES:

- 1) Duncan, C., Smith, A. E., and Aguirre, F. H., "Iris Transponder – Communications and Navigation for Deep Space," 2014 AIAA/USU Conference on Small Satellites, #SSC14-IX-3 (<http://digitalcommons.usu.edu/cgi/viewcontent.cgi?article=3083&context=smallsat>)
- 2) Howard, R.A., Moses, J.D., Vourlidis, A., Newmark, J.S., Socker, D.G., Plunkett, S.P,

- Korendyke, C.M., Cook, J.W., Hurley A., Davila, J.M., Thompson, W.T., O.C. St Cyr, C., Mentzell, E., Mehalik, K, Lemen, J.R., Wuelser, J.P., Duncan, D.W., Tarbell, T.D., Wolfson, C.J., Moore, A., Harrison, R.A., Waltham, N.R. , Lang, J., David, C., Eyles, C.J., Mapson-Menard, H., Simnett, G.M., Halina, J.P., Defise, J.M., Mazy E., Rochus, P., Mercier, R., Ravet, F., Delmotte, F., Auchere, F., Delaboudineiere, J.P., Bothmer, V., Deutsch, W., Wang, D., Rich, N., Cooper, S., Stephens V., Maahs, G., Baugh, R., McMullin, D., Carter, J.T., “Sun Earth Connection Coronal and Heliospheric Investigation (SECCHI)”, *Space Science Review* (2008) 136: 67-115.
- 3) Michels, D.J., Howard, R.A., Koomen, M.J. and Sheeley, N.R. Jr., “Satellite observations of the outer corona near sunspot maximum”, in *Radio Physics of the Sun*, edited by M.R. Kundu and T.E. Gregeley, *Sym. Int. Astron. Union*, 86, 439-442, 1980.
- 4) Korendyke, C. M., Vourlidas, A. Plunket, S.P., Howard, R.A., Wang, Dennis, Marshall, C.J., Waczynski A., Janesick, J. Elliot, T., Tun, S., Tower, John R., Grygon, M., Keller, D. and Clifford, G.E., *Development and test of an active pixel sensor detector for Heliospheric Imager on Solar Orbiter and Solar Probe Plus*, SPIE, 8862, 2013, DOI:10.1117/12.2027655.
- 5) Liewer, P.C., Klesh, A.T., Lo, M.W., Murphy, N., Staehle, R.L., Angelopoulos, V., Anderson, B.D., Aray, M., Pellegrino, S., Cutler, J.W., Lightsey, E.G., Vourlidas, A. “A fractionated Space Weatehr Base at L5 using CubeSats and Solar Sails, in *Advances in Solar Sailing Vol. 1*, Macdonald, Malcolm (Ed.), *Spring Praxis Books*, Springer-Verlag Berlin Heidelberg, (2014), p. 269.